

DOI: 10.1002/cbic.200700229

Dynamic Conformational Behavior and Molecular Interaction Discrimination of DNA/Binder Complexes by Single-Chain Stretching in a MicroDevice

Wei-Hua Huang,^[a] Anatoly A. Zinchenko,^[b]
Cyril Pawlak,^[a] Yong Chen,^[a] and Damien Baigl^{*[a]}

The compaction of DNA is an essential step in several biological applications, including gene delivery.^[1] During the past two decades many studies have been devoted to the *in vitro* compaction of DNA, and various compaction agents have been identified, such as polycations, multivalent metal cations, hydrophilic polymers and surfactants.^[2] The manipulation of the unfolding and folding of DNA is considered to be a key to controlling its biological activity. On the other hand, it is known that DNA molecules can be "stretched" from the random coil to an elongated state^[3] by using microfluidic or electrodynamic methods.^[4] However, such an approach has never been applied to DNA in a compact state. In this communication, we report on the use of a microfluidic device to study the unfolding process of compact single-chain DNA and its relationship with the molecular interaction between DNA and compaction/binding molecules.

For the DNA-stretching experiments, we constructed a microdevice as illustrated in Figure 1 A. It is a polydimethylsiloxane (PDMS) microfluidic chip that contains two crossing channels (1 μm height) with PDMS micropillars inside the main channel (Figure 1 A and B); these are bound to a microscopy glass cover slide. A voltage difference (DC) was applied for DNA injection (E_4 – E_2) or DNA migration (E_3 – E_1). The DNA molecules were in the coil state when they migrated into the main channel, but once a DNA molecule entered the micropillar region, the additional friction force with the micropillar obstacles induced the stretching of the molecule (Figure 1 C). Similar stretching behavior has been found during DNA separation in a sieving medium, such as polymers^[3d] or nanostructures.^[5] In our case, the hydrodynamic force was enough to stretch the DNA partially in the micropillar region, but the stretching was much more efficient when it was coupled with an electrodynamic force; this is in agreement with previous results on DNA separation through deterministic lateral displacement by using

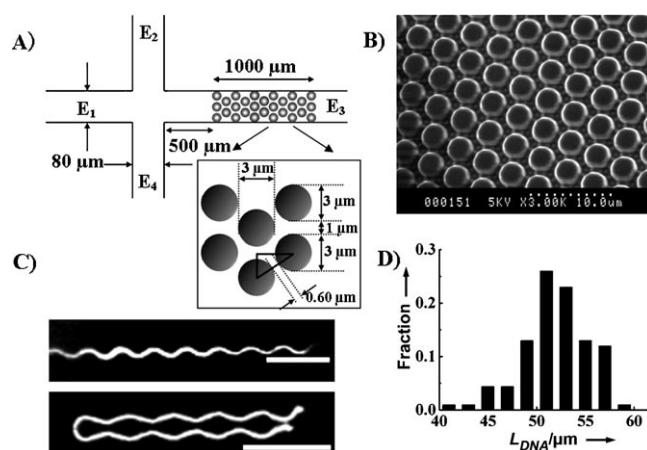


Figure 1. A) Schematic representation of a microdevice with micropillars for DNA stretching and unfolding. B) SEM image of the micropillars in the main channel. Micropillars (1 μm height, 3 μm diameter) were made in polydimethylsiloxane (PDMS) and separated by a distance of 1 μm . C) Fluorescence microscopy (FM) pictures showing the stretching states of two individual DNA molecules under an electric field of 10 V cm^{-1} . D) Length distribution of stretched T4 DNA molecules under an electric field of 10 V cm^{-1} . The averaged stretching length is $52.0 \pm 0.3 \mu\text{m}$. Scale bars are 10 μm .

micropillars as obstacles.^[6] For electric fields greater than 5 V cm^{-1} , most of the DNA molecules were highly stretched (Figure 1 C, top and movie in the Supporting Information), and they were nearly fully stretched when they adopted the typical U shape (Figure 1 C, bottom). At 10 V cm^{-1} , we observed that 89% of the individual DNA molecules were stretched up to an apparent length of 48–58 μm (full distribution in Figure 1 D), which is comparable to the T4 contour length (57 μm).

By using fluorescence microscopy (FM), we have studied the bulk conformation of a large number of individual T4 DNA molecules (0.1 μm in Tris–HCl buffer) in the presence of two different compaction agents: 1) spermine (SPM), a natural tetraamine; and 2) poly(L-lysine) (PL), a polycation with ammonium groups as positive charges. In the presence of SPM, we found that all of the DNA molecules were in the coil state at a low SPM concentrations (Figure 2 A, left), but at a higher SPM concentration they were in a fully compact state (Figure 2 A, right). For intermediate SPM concentrations, there was no intermediate state, and both the coil and compact states coexisted (Figure 2 A, middle); in this region, the fraction of compact states increased when the SPM concentration increased (Supporting Information). Figure 2 C shows the long-axis length of DNA (L_{DNA}), which averaged about 200 individual molecules. Three regions were clearly identified: a coil state ($L_{\text{DNA}} = 2.7 \pm 0.4 \mu\text{m}$, $[\text{SPM}] < 4.5 \mu\text{M}$), a coexistence region ($4.5 \leq [\text{SPM}] \leq 6 \mu\text{M}$) and a fully compact state ($L_{\text{DNA}} = 0.8 \pm 0.1 \mu\text{m}$, $[\text{SPM}] > 6 \mu\text{M}$). Furthermore, one notes that the minimal SPM concentration to get all the DNA molecules into compact states is about 6 μM , which corresponds to a SPM/DNA charge ratio of about 240:1 (spermine concentration thus acts as an environmental parameter). Finally, the DNA folding transition is a reversible process, and the unfolding of DNA that had been compacted by spermine was obtained by adding a monovalent salt, or by diluting the SPM concentration. All these features are characteristic of a first-order phase transition at the

[a] Dr. W.-H. Huang, C. Pawlak, Prof. Y. Chen, Dr. D. Baigl
Department of Chemistry, Ecole Normale Supérieure
24 rue Lhomond, 75005 Paris (France)
Fax: (+33) 1-4432-2402
E-mail: damien.baigl@ens.fr

[b] Dr. A. A. Zinchenko
Graduate School of Environmental Studies, Nagoya University
Chikusa, Nagoya 464-8601 (Japan)

Supporting information for this article is available on the WWW under <http://www.chembiochem.org> or from the author.

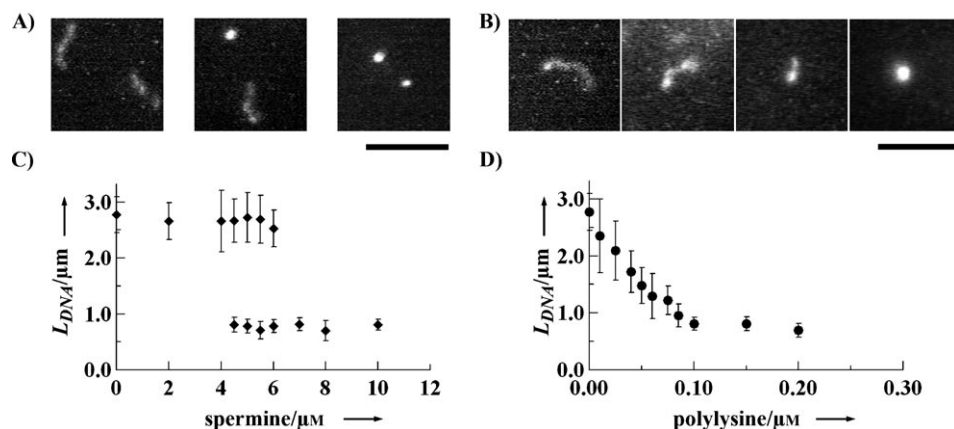


Figure 2. Single-chain characterization of duplex T4 DNA ($0.1 \mu\text{M}$ in 10 mM Tris-HCl buffer), labeled by DAPI ($0.1 \mu\text{M}$) in the presence of spermine and PL. A) Typical FM images of T4 DNA in the bulk solution for an increasing concentration of spermine (from left to right: 0 , 5 , and $10 \mu\text{M}$). B) Typical FM images of T4 DNA for an increasing concentration of PL (from left to right: 0 , 0.02 , 0.04 , and $0.1 \mu\text{M}$). DNA long-axis length averaged on ca. 200 individual molecules of T4 DNA as a function of C) spermine and D) PL concentration. Scale bars are $5 \mu\text{m}$.

DNA single-chain level,^[7] and they can be explained by the ion exchange between DNA–monovalent and DNA–multivalent (here spermine) counter ion species; the transition occurs at a DNA charge neutralization of $88\text{--}90\%$.^[8] In contrast, we found that when DNA is compacted by a long polycation, for instance PL with a molecular weight $30\,000\text{--}70\,000 \text{ g mol}^{-1}$, the nature of the molecular interaction is different. Between the DNA coil state in the absence of PL, and the fully compact state at a PL concentration of $0.1 \mu\text{M}$, intermediate states could be observed with a degree of compaction that increases when PL increases (Figure 2B). Figure 2D shows L_{DNA} averaged on about 200 individual DNA molecules as a function of PL concentration. Contrary to the typical all-or-none behavior shown in Figure 2C, L_{DNA} decreases continuously from 2.7 to $0.8 \mu\text{m}$ as the PL concentration increases from 0 to $0.1 \mu\text{M}$. Moreover, all of the DNA molecules are in the fully compact state at PL concentrations greater than $0.1 \mu\text{M}$, which corresponds to a PL/DNA charge ratio of approximately $1:1$. This $1:1$ charge binding is entropically favorable due to the important release of counter ions through complexation. Finally, once DNA was compacted by the addition of PL, it could not be unfolded by PL dilution. All these features show that the mechanism of DNA compaction is based on a strong inter-polyelectrolyte complexation mechanism^[9] between DNA and PL molecules.

We showed that compact DNA molecules can be obtained by considering two different mechanisms of molecular interactions: reversible ion-exchange or irreversible interpolyelectrolyte complexation. We have thus studied the consequence of these two mechanisms on the stretching behavior of compact DNA molecules in our microdevice. We observed that under hydrodynamic/electrodynamic force, DNA molecules that had been compacted by spermine can be dynamically unfolded under constant chemical composition of the medium ($[\text{SPM}] = 10 \mu\text{M}$, salt concentrations, buffer composition and dielectric constant are constant). The compact DNA molecules showed repeatedly the following sequence of conformation changes—

unfolding, stretching, and compacting—when they migrated through the micropillars (Figure 3A and movies in the Supporting Information). This unfolding process at a constant chemical composition is only possible because of the reversible nature of the DNA compaction by small multivalent counter ions.

There were two main differences between DNA in the coil state and DNA in the compact state regarding their single-chain stretching behaviors. First, while a hydrodynamic force was enough to stretch the DNA molecules partially in the coil state, the DNA molecules in the com-

compact state could not be unfolded in the absence of an electric field, which shows that a stronger force is needed to unfold compact DNA than stretching DNA from a coil state. Moreover, the averaged stretched length of individual molecules of DNA in the compact state was less than that of coiled DNA under the same electric field, especially under a moderate electric field ($< 20 \text{ V cm}^{-1}$). Figure 3B and C show that the averaged stretched length of individual DNA molecules that had been compacted by spermine increases from 12.1 to $38.8 \mu\text{m}$ when the applied electric field increases from 5 to 50 V cm^{-1} . We also investigate the influence of the SPM concentration on the unfolding process of compact DNA molecules. We found that T4 DNA that had been compacted with higher SPM concentrations ($20\text{--}50 \mu\text{M}$) could also be unfolded. However, the electric field that was required to obtain a given unfolded length increased strongly with an increase in SPM concentration (Figure 3D). All these experimental findings are in agreement with the results from single-chain stretching by optical tweezers by Bauman et al., who revealed the significant decrease of the persistence length with an increase in condensing agent concentration.^[10] Furthermore, because compact DNA molecules under bulk conditions are typically 100 nm in diameter,^[2b,11] we could have expected that most of the compact DNA molecules would go freely through the intervening space between micropillars ($600 \text{ nm}\text{--}1 \mu\text{m}$) with very few stretching sequences. In contrast, we observed that almost all of the compact DNA molecules were significantly stretched when they migrated through micropillars. This can be explained by the fact that compact DNA molecules were partially unfolded or stretched when they migrated in the channel under the electric field before entering the micropillar region. By fluorescence microscopy, we measured an averaged long-axis length of $1.5 \pm 0.5 \mu\text{m}$ in the channel before the micropillar region while under bulk conditions the averaged long-axis length was $0.8 \pm 0.1 \mu\text{m}$; this corresponds well to a size of $0.1\text{--}0.2 \mu\text{m}$ if we take into account the blurring effect of fluorescence light.^[12] Then, we performed the same experiment with polylysine as a com-

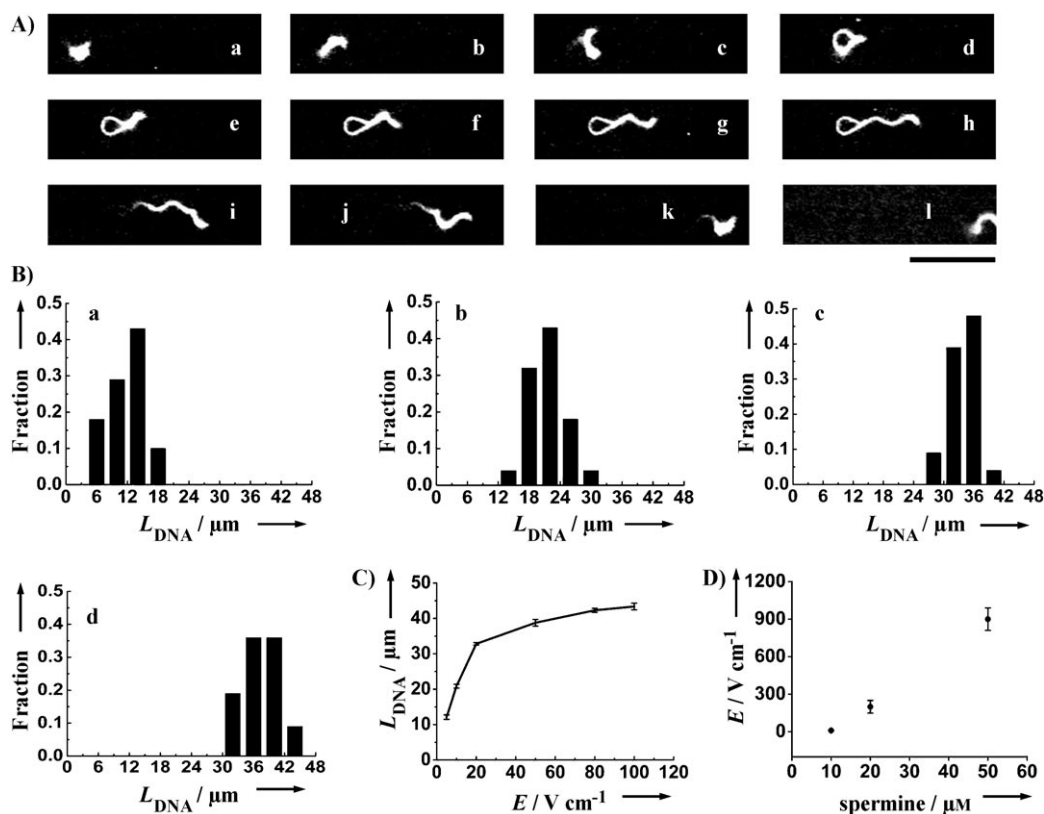


Figure 3. DNA compacted by spermine. A) Consecutive FM images (every 0.17 s) showing the kinetic unfolding and stretching processes of a single DNA molecule under an electric field of 20 V cm^{-1} . Scale bar is $10 \mu\text{m}$. B) Length distributions and C) averaged length of unfolded DNA molecules under different electric fields E (the electric fields in (B) for a, b, c, d are 5, 10, 20, 50 V cm^{-1} , respectively). D) Electric field E necessary to obtain an averaged DNA unfolding length of $20 \mu\text{m}$ as a function of spermine concentration. For all experiments, the T4 DNA concentration was $0.1 \mu\text{M}$. The spermine concentration was $10 \mu\text{M}$ in (A)–(C).

paction agent instead of spermine. Figure 4A shows a typical FM picture of DNA molecules that were compacted by $0.1 \mu\text{M}$ PL in the micropillar region under an electric field of 100 V cm^{-1} . In this picture, all of the DNA molecules appear as compact globules. By varying the electric field, the same observation was made, and we found that all of the DNA molecules that had been compacted by PL stayed in the compact state without unfolding or stretching regardless of the applied electric field between 0 and 1000 V cm^{-1} (Figure 4B). This behavior is strikingly different from that of DNA that had been compacted by spermine and can be interpreted as a consequence of

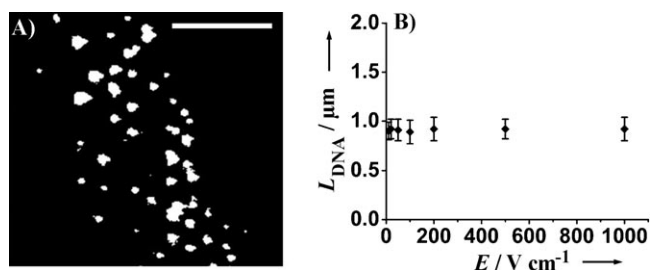


Figure 4. DNA compacted by PL. A) FM image of DNA molecules compacted by poly(L-lysine) under an electric field of 100 V cm^{-1} . Scale bar is $10 \mu\text{m}$. B) DNA long-axis length averaged on ca. 200 individual molecules as a function of electric field. For all experiments the T4 DNA concentration was $0.1 \mu\text{M}$ and the PL concentration was $0.1 \mu\text{M}$.

the strong interpolyelectrolyte complexation mechanism between DNA and PL molecules.

Finally, it is interesting to consider the relationships between DNA molecular interactions, compaction mechanism, and unfolding properties by single-chain stretching. In the case of low-molecular-weight, oppositely charged, multivalent counter ions (e.g., spermine), the compaction is mainly driven by the neutralization of the DNA charge by the counter ions. Many counter ions localize in the vicinity of the chain where the electrostatic potential is very high (Poisson–Boltzmann). However, these counter ions are not permanently bound to the chain: they exchange dynamically with the bulk ions and keep the translational entropy along the chain high. DNA molecules that had been compacted by such a process can thus be stretched with a sufficiently high stretching force. In contrast, in the presence of oppositely charged high-molecular polyelectrolytes, for example, polylysine, DNA molecules form interpolyelectrolyte complexes, in which a very large number of strong Coulomb bounds are formed between oppositely charged monomers. This might explain the irreversible character of the compaction transition under bulk conditions, as well as our inability to stretch DNA molecules that had been compacted by polylysine in our microdevice even under high electric fields.

In conclusion, we have used a microdevice to discriminate the molecular interaction mechanism between DNA and com-

paction agents by stretching and unfolding single-chain DNA under hydrodynamic/electrodynamic forces. It has been found that DNA molecules that had been compacted by spermine could be dynamically unfolded because the compaction resulted from reversible ion-exchange and a first-order folding transition.^[7,8] In contrast, DNA molecules that had been compacted by polylysine could not be unfolded due to the mechanism of strong interpolyelectrolyte complexation. The developed methodology and the results obtained might find applications for the separation of large DNA molecules and for the stability screening of DNA–binder complexes. Furthermore, this method enables the dynamic control of DNA conformation, which can be used locally to regulate the bioactivity of DNA at the level of a single DNA molecule.

Experimental Section

Microdevice fabrication: Standard UV Photolithography was used to generate the mold for the microfluidic chip. Briefly, an AZ 5214E photoresist (Clariant, Paris, France) was first spin coated to a final height of 1 μm on a silicon wafer, prior to exposure to a 1 μm -resolution Cr mask under a UV light and development in AZ 726 MIF developer (Clariant). Soft lithography was then used to replicate the PDMS microfluidic device. The silicon wafer was pretreated with trimethylchlorosilane vapor (TMCS) to prevent cured PDMS from sticking to the wafer. After pouring, the RTV 615 PDMS (General Electric, A and B components were mixed in the ratio of 10:1) was allowed to degas before curing at 80 °C for 1 h. The cured PDMS was peeled off from the master, and small holes were then drilled for the reservoirs in the PDMS. The final microdevice was assembled by bonding the PDMS structures on a glass cover slide, both treated by oxygen plasma. Figure 1A shows the final structure of the microdevice. Figure 1B shows a scanning electron microscopy (SEM) image of the PDMS micropillars.

Fluorescence microscopy: FM observations were performed by using Axiovert 135 TV and Axiovert 200 (Carl Zeiss) inverted microscopes that were equipped with a 100 \times oil-immersed objective lens. Images were captured by using an EB-CCD camera and a SIT camera (C2400–08) from Hamamatsu photonics (Hamamatsu, Japan), respectively. Data were recorded and analyzed (including DNA size determinations) by Scion Image and Image J image-processing softwares.

DNA single-chain observations in the bulk solution: Very dilute T4 DNA solutions (0.1 μM in nucleotides) were prepared in Tris–HCl buffer (10 mM, pH 7.4) by adding carefully DNA to a solution that contained Tris–HCl buffer, DAPI (4'6-diamidino-2-phenylindole, final concentration 0.1 μM), and spermine tetrahydrochloride (SPM) or poly(L-lysine) of molecular weight 30000–70000 (PL). Samples were placed in custom-built microscope cells, and observed by fluorescence microscopy. Under these experimental conditions, we could directly observe the bulk conformation of a large number of individual DNA chains. The coil and full compact states of individual chains were clearly distinguishable: compared to full compact DNA, which appeared as a bright fast-diffusing spot, DNA in the coil state had a much larger apparent long-axis length (longest distance in the outline of the DNA image), a much lower translational diffusion coefficient, and exhibited characteristic intra-chain thermal fluctuations. Intermediate states corresponded to fluctuating chains with a long-axis length smaller than the typical long-axis length of DNA in a coil state ($2.7 \pm 0.4 \mu\text{m}$ under our experimental conditions)

DNA stretching: DNA solutions (0.1 μM in nucleotides) were prepared in 0.5 \times TBE electrophoresis buffer (45 mM Tris–borate, 1 mM EDTA, pH 8.0) that contained 4% (v/v) 2-mercaptoethanol to reduce photobleaching, and the DNA was stained with YOYO-1 (Quinolinium, 1,1'-[propane-1,3-diylbis[[dimethyliminio]propane-3,1-diyl]]bis[4-[(3-methyl-2(3*H*)-benzoxazolylidene)methyl]] tetraiodide, final concentration 0.01 μM) for fluorescence microscopy observation. The microdevice was filled with the buffer solution, which also contained the condensing agents (spermine or polylysine) for the experiments on DNA unfolding. A voltage difference (DC) was applied between E4 and E2 for DNA injection, and between E3 and E1 for DNA migration. Individual DNA molecules in the microdevice were observed by fluorescence microscopy.

Acknowledgements

This work was partially supported by ICORP "Spatio-Temporal Order" project, JST (Japanese Science and Technology Agency), the Centre National de la Recherche Scientifique (CNRS), and the European Commission through project NMP4-CT-2003-505311 (Nabis).

Keywords: compaction · DNA structures · microfluidics · stretching · unfolding

- [1] D. Luo, W. M. Saltzman, *Nat. Biotechnol.* **2000**, *18*, 33–37.
- [2] a) V. A. Bloomfield, *Curr. Opin. Struct. Biol.* **1996**, *6*, 334–341; b) L. C. Gosule, J. A. Schellman, *Nature* **1976**, *259*, 333–335; c) U. K. Laemmli, *Proc. Natl. Acad. Sci. USA* **1975**, *72*, 4288–4292; d) J. Widom, R. L. Baldwin, *Biopolymers* **1983**, *22*, 1595–1620; e) S. M. Mel'nikov, V. G. Sergeyev, K. Yoshikawa, *J. Am. Chem. Soc.* **1995**, *117*, 2401–2408; f) A. A. Zinchenko, K. Yoshikawa, D. Baigl, *Phys. Rev. Lett.* **2005**, *95*, 228101.
- [3] a) S. B. Smith, Y. Cui, C. Bustamante, *Science* **1996**, *271*, 795–799; b) X. Michalet, R. Ekong, F. Fougereuse, S. Rousseaux, C. Schurra, N. Hornigold, M. Slegtenhorst, J. Wolfe, S. Povey, J. S. Beckmann, A. Bensimon, *Science* **1997**, *277*, 1518–1523; c) S. Ferree, H. W. Blanch, *Biophys. J.* **2004**, *87*, 468–475; d) G. C. Randall, K. M. Schultz, P. S. Doyle, *Lab Chip* **2006**, *6*, 516–525.
- [4] a) S. Ferree, H. W. Blanch, *Biophys. J.* **2003**, *85*, 2539–2546; b) R. Riehn, M. Lu, Y. M. Wang, S. F. Lim, E. C. Cox, R. H. Austin, *Proc. Natl. Acad. Sci. USA* **2005**, *102*, 10012–10016.
- [5] a) J. Han, H. G. Craighead, *Science* **2000**, *288*, 1026–1029; b) P. S. Doyle, J. Bibette, A. Bancaud, J.-L. Viovy, *Science* **2002**, *295*, 2237; c) N. Kaji, Y. Tezuka, Y. Takamura, M. Ueda, T. Nishimoto, H. Nakanishi, Y. Horiike, Y. Baba, *Anal. Chem.* **2004**, *76*, 15–22.
- [6] L. R. Huang, E. C. Cox, R. H. Austin, J. C. Sturm, *Science* **2004**, *304*, 987–990.
- [7] K. Yoshikawa, M. Takahashi, V. V. Vasilevskaya, A. R. Khokhlov, *Phys. Rev. Lett.* **1996**, *76*, 3029–3031.
- [8] a) R. W. Wilson, V. A. Bloomfield, *Biochemistry* **1979**, *18*, 2192–2196; b) D. Baigl, K. Yoshikawa, *Biophys. J.* **2005**, *88*, 3486–3493.
- [9] V. A. Kabanov, V. G. Sergeyev, O. A. Pyshkina, A. A. Zinchenko, A. B. Zezin, J. G. H. Joosten, J. Brackman, K. Yoshikawa, *Macromolecules* **2000**, *33*, 9587–9593.
- [10] C. G. Baumann, V. A. Bloomfield, S. B. Smith, C. Bustamante, M. D. Wang, S. M. Block, *Biophys. J.* **2000**, *78*, 1965–1978.
- [11] a) N. V. Hud, K. H. Downing, *Proc. Natl. Acad. Sci. USA* **2001**, *98*, 14925–14930; b) C. C. Conwell, I. D. Virfan, N. V. Hud, *Proc. Natl. Acad. Sci. USA* **2003**, *100*, 9296–9301.
- [12] K. Yoshikawa, Y. Matsuzawa, *Phys. D* **1995**, *84*, 220–227.

Received: May 2, 2007

Published online on September 13, 2007